

EMULATE Deliverable D13: Assessment of the relative influence of external forcing factors (natural and human) and internal variability and their seasonal differences

Hadley Centre (Partner 2), UBERN (partner 6).

Jeff Knight¹, Adam Scaife¹, David Fereday¹, Chris Folland¹, and Elena Xoplaki²

¹- Hadley Centre, Met Office, UK.

²- University of Bern, Switzerland.

1. Introduction

This deliverable report is concerned with the parts of WP3 of the EMULATE project aimed at using ensembles of climate model simulations to infer the contributions of natural and anthropogenic external forcing factors and internal variability on European climate, with a particular focus on circulation regimes. It relates to the results reported in various other EMULATE deliverables. This is firstly through the use of the circulation classification derived in WP2, and secondly by extending the results of D12, which tests whether the model simulations reproduce the observed variability described in D7 and D11.

It is crucial in informing efforts to mitigate and adapt to possible future climate change to understand the full attribution of changes in past climate, regardless of their cause. Only by this means can climate projection models be tested and so give confidence in their predictions of the future (e. g. Stott *et al.*, 2000). By studying the causes of past variability we may learn what future climate changes can be influenced, what variability the unmodified climate system can produce, and what the climatic response to future natural forcing events (such as volcanic eruptions) will be.

On regional scales, such as the North Atlantic-European area studied in EMULATE, changes in circulation are of paramount importance for understanding climate variability. This is in contrast to global mean climate, which is more closely tied to the overall radiative balance of the atmosphere. Regional climatic responses could be significantly modified dependent on whether part of that response is a change in circulation (Scaife *et al.*, 2005). In our regional framework, therefore, we examine the effect of climate forcings on circulation. To do this, we use the circulation classification developed in WP2 of EMULATE, which, as will be shown, can be applied to the results from the EMULATE simulations.

The climate model used in EMULATE is HadAM3, the third version of the Hadley Centre atmospheric climate model (Pope *et al.*, 2000). Our simulations are forced by interpolated monthly sea-surface temperature and sea-ice concentrations from the HadISST1 data set (Rayner *et al.*, 2003), which is an analysis of observed marine data from 1870. We perform two ensembles, called 'natural forcings' and 'all forcings', each with 6 members simulating 1870-2002, plus an additional 12 members simulating 1950-2002. The 'natural' ensemble includes the major natural forcing factors - Milankovitch forcing, solar forcing and volcanic forcing. The 'all forcings' ensemble includes these forcings plus the major

anthropogenic forcings - well-mixed greenhouse gases, direct and indirect forcings by anthropogenic sulphate aerosols, tropospheric and stratospheric ozone changes and land-use changes. The data used to specify these forcings are described in Stott *et al.* (2000) and Johns *et al.* (2003), except for the Milankovitch and land-use changes. The Milankovitch forcing represents the effects of the slow changes in terrestrial precession, obliquity and orbital eccentricity and is small over the time scales of the EMULATE ensembles. The land-use forcing represents changes in a variety of surface characteristics, such as deep-snow albedo and the roughness length (R. Betts, personal communication).

The total forcing from all factors in the natural and all forcings ensembles is shown for the global mean and the European area mean in figure 1. All the diagnosed forcings show a large but short-lived negative response to volcanic eruptions. Taking this into account, both the global and European natural ensemble forcings show relatively little long term change - much less than 0.5 W m^{-2} . The global mean forcing in the all forcings ensemble is always greater than that in the natural ensemble, and grows from about $+0.2 \text{ W m}^{-2}$ to over $+2 \text{ W m}^{-2}$ between 1870 and 2002. In contrast, the European mean forcing in the all forcings case is always less than that in the natural ensemble, decreasing from about -0.5 W m^{-2} in 1870 to almost -3 W m^{-2} in the 1960s, and then increasing to about -0.5 W m^{-2} again by 2002. The smoothed difference between the natural and all forcings ensembles (i.e. the anthropogenic component) mirrors very closely the low-frequency component of the all forcings ensemble in each case.

These forcings can be explained by the relative contributions of greenhouse-gases (which trap terrestrial infrared radiation and act as a positive forcing) and sulphate aerosols (which reflect solar radiation and act as a negative forcing). Both are a product of industrial societies, but aerosols are short-lived and remain relatively close to their source, whereas greenhouse-gases persist for years to centuries - long enough for them to become evenly mixed through the atmosphere. As a result of Europe's industrial history, which more than spans the period of our ensembles, historical aerosol amounts are, therefore, much higher than in most other parts of the world, yet greenhouse gas concentrations are similar everywhere. Hence on the global scale the positive effect of greenhouse-gases outweighs the regional negative effect of aerosols. For Europe, however, the reverse appears to be true, giving rise to the perhaps unfamiliar situation of anthropogenic forcing being negative between 1950 and 2000. The growing influence of greenhouse-gases, and efforts to reduce aerosol pollution in Europe, have resulted in a turn-round in the negative trend in forcing from about the 1960s. Overall, therefore, European forcing levels in the all forcings simulations are almost the same as those in the natural simulations by 2002.

The effect on these forcing differences on simulated annual mean European temperature is shown in figure 2. Both ensembles reproduce the shape of the observed global mean temperature curve (see e.g. Folland *et al.*, 2001), with increasing temperatures in the early and late 20th century separated by a cooling period. The statistical comparison of the two ensembles shows that having more ensemble members after 1950 reduces the range of differences for which the ensemble means are statistically consistent. This is so much so that before 1950 there are no significant differences in

European annual mean temperature between the two ensembles. In contrast, between 1950 and about 1980, the all forcings ensemble is significantly cooler, by about 0.6 °C, than the natural forcings ensemble. After 1980, the two ensembles become consistent again, despite the increased ability of the large ensemble size to resolve differences. The relative cooling in the all forcings ensemble mirrors the relative negative climate forcing; both forcing and temperature differences show negative trends until about 1960 and then increase to about zero by 2002. As such, this cooling is clearly a result of the anthropogenic aerosol included in the model. Combining the peak cooling and peak forcing values implies a regional climate sensitivity of just a few tenths of a °C per W m^{-2} . This is much smaller than values usually discussed in the global context and presumably reflects the moderating influence of heat transport to Europe from other regions which warmed more continuously. Large interannual variability in European temperatures prevents the use of observations to discriminate between the ensembles.

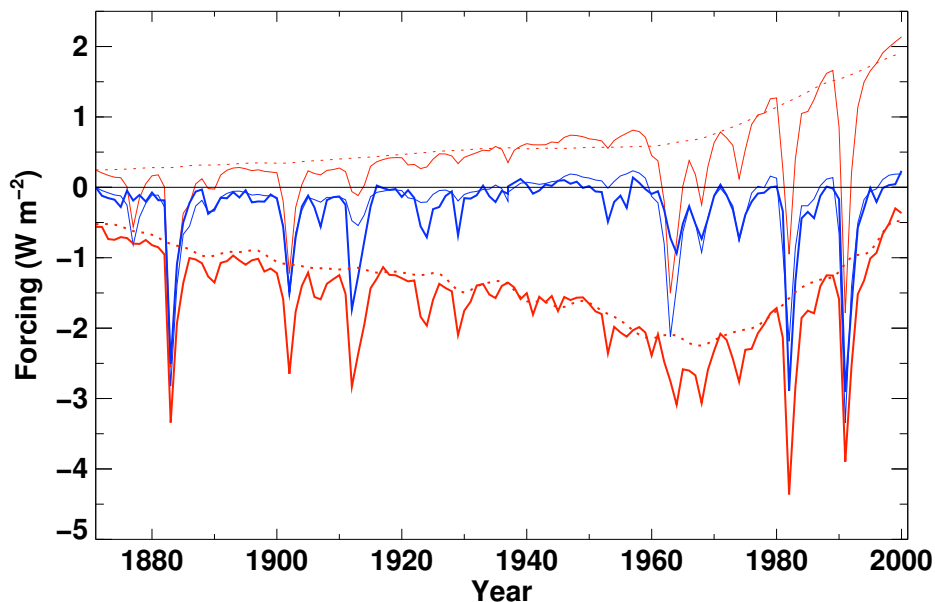


Figure 1 Global and European ($25^{\circ}\text{W}-60^{\circ}\text{E}$, $36^{\circ}-72^{\circ}\text{N}$) area mean total forcing in the EMULATE ensembles. The global forcings are shown as thin solid curves, with blue representing the natural ensemble and red representing the all forcings ensemble. The thin dashed curve is the low-frequency component of the difference in forcing between all forcings and natural ensembles. An equivalent set of thick curves represent the European area mean forcing. Values are plotted relative to the 1870 forcing value in the natural ensemble in each case. Note the forcings here are for the tropopause and instantaneous changes, i.e. without atmospheric adjustment.

2. Simulated effect of anthropogenic forcings on European mean climate: 1951-2000

In the previous section it was shown that the all forcings ensemble was significantly cooler in the annual mean than the natural ensemble only after 1950. As a result the focus will be on

the post-1950 period in further analyses to take advantage of the larger ensemble size during the latter parts of the ensembles. We compare the spatial distribution of differences to the mean climate of the 1951–2000 period between the ensembles for the 6 two-month seasons of the year. These are defined as January–February (JF), March–April (MA), May–June (MJ), July–August (JA), September–October (SO), and November–December (ND). The variables for comparison are surface air temperature, mean sea-level pressure (mslp) and precipitation.

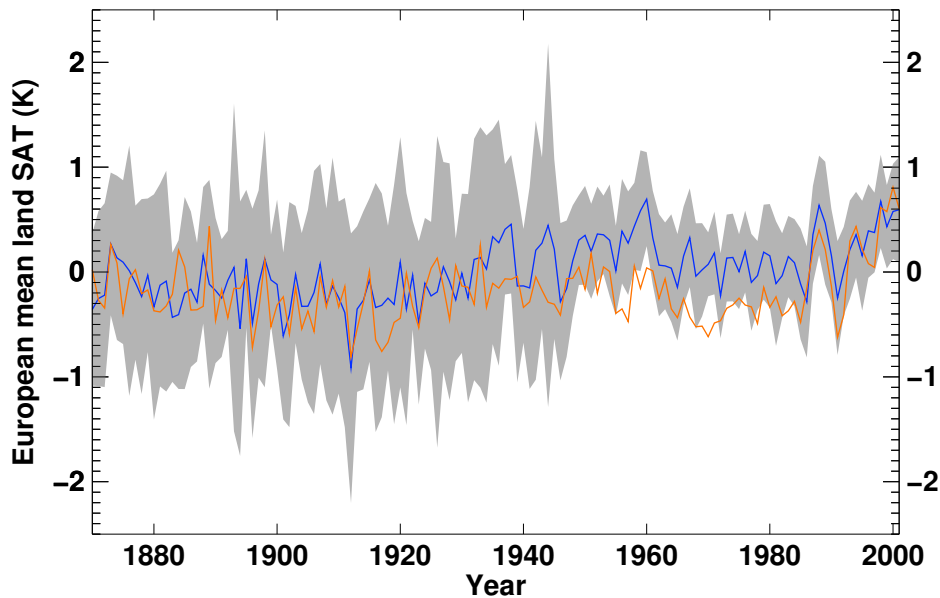


Figure 2 Mean European (as defined in figure 1) annual land surface air temperature anomalies (relative to the mean 1871–2002 temperature in the natural ensemble). The ensemble mean value for the natural ensemble is shown in blue and the equivalent for the all forcings is in red. Grey shading represents the 95% significance limits of the difference between the ensemble means centred on the natural ensemble mean.

(a) Surface Temperature

Surface temperature differences show a seasonal split between the warm and cool parts of the year (figure 3). In JF, the all forcings ensemble is significantly cooler than the natural ensemble over Eastern Europe, by up to 1 °C or more. Over northern Scandinavia, the all forcings ensemble is warmer. The difference is even larger in MA, with the relative cold extending to Western Europe. MJ, JA and SO do not show as large negative differences over Eastern Europe, but show a more general European coolness, with the largest changes in Southern Europe. ND has a pattern of coolness over Eastern Europe with warmth in Scandinavia, resembling the patterns of JF and MA, but with a smaller amplitude.

The seasonality of these changes reflects the forcing that acts to create them. Although aerosol amounts do not vary greatly through the year, the amount of solar radiation they reflect is much greater in summer than in winter. Consequently, in the cool

seasons, aerosol cooling appears to only affect regions where temperature changes are amplified by increases in snow cover e.g. Eastern Europe. In contrast, in the warm seasons, aerosol cooling is more general and largest over regions at lower latitudes and with small cloud amounts e.g. Southern Europe. The seasonal reversal of the anthropogenic effect in Scandinavia - showing warming in winter and cooling in summer - reflects the fact that with such limited sunlight, aerosols have no effect at high latitudes in winter.

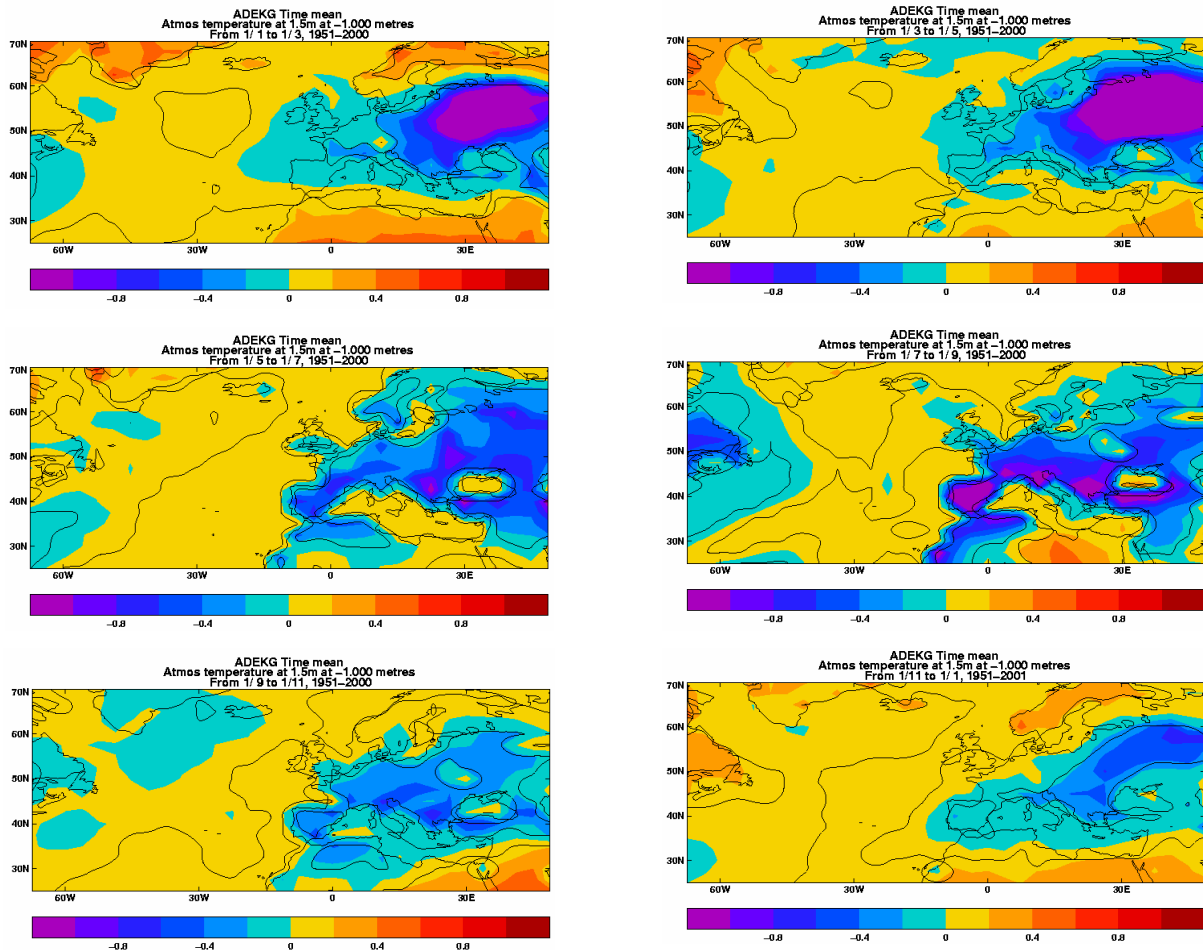


Figure 3 Mean 1951-2000 surface air temperature differences between the two ensembles for the six two-month seasons. Top row: JF (left) and MA (right), middle row: MJ (left) and JA (right), bottom row: SO (left) and ND (right). Units are °C. Solid contours bound regions where the ensembles differ at the 90% confidence level.

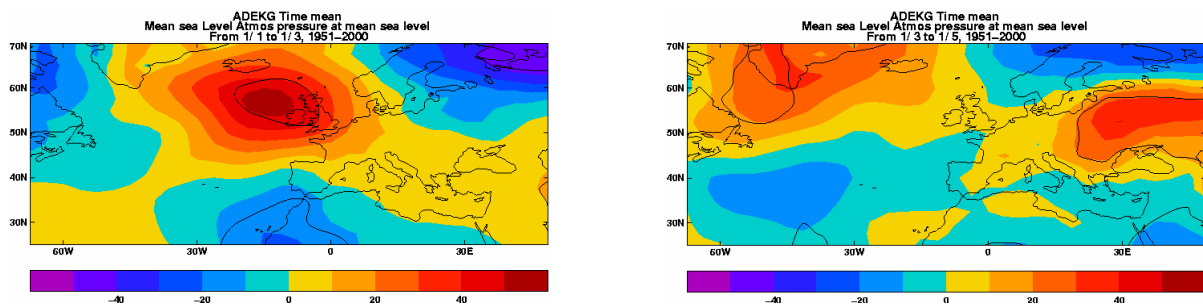
(b) Mean Sea-Level Pressure

The differences between natural and all forcings mean 1951-2000 mslp also show marked season variations (figure 4). In JF the only significant differences in the all forcings ensemble relative to natural ensemble are increased anticyclonicity north-west of the British Isles and lower pressure over North Africa. There does not appear to be any projection of this pattern onto the leading modes of wintertime variability such as the North Atlantic Oscillation (NAO). Similarly, MA has only limited changes, with higher pressure over Eastern Europe. For MJ and JA a different pattern emerges. Here, there appears to be an anthropogenic reduction in mslp over the North Atlantic Ocean and North West Europe that is

similar to the southern node of the negative phase of the summer NAO – the principal mode of year to year circulation variability in JA (see D7). In addition, there is again higher pressure in Eastern Europe in the all forcings ensemble, as well as higher pressure over the Iberian Peninsula. SO has a negative mslp difference over much of the northern North Atlantic, with positive differences at lower latitudes and in Eastern Europe. ND is similar to JF in having limited significant differences, with a positive mslp difference to the west of Europe. Overall, the size of these changes is small (up to ~ 0.5 hPa) compared to year-to-year variations. These are, however, 50-year mean differences, so even these small biases could be important. The largest and most significant effects are seen in summer, as lower internal variability leads to a higher ratio between the anthropogenic forcing signal and noise.

(c) Precipitation

Changes in long-term average precipitation are often related to mslp changes. This tends to be the case for the differences between mean precipitation in the two ensembles (figure 5). In JF, the all forcings precipitation is lower than that in the natural over North West Europe, in line with the significant anticyclonic anomaly there. There are additional rainfall reductions over North East Europe. This is liable to arise due to the circulation in the all forcings ensemble advecting more cold, dry polar air (figure 4). MA has an anthropogenic signal of less precipitation over most of Europe apart from southernmost regions. This Southern European signal for more rainfall is more pronounced in MJ, while less precipitation remains over Northern Europe. In contrast, JA has increased precipitation in the all forcings case for much of Western and Southern Europe, with only Northeastern Europe showing less. The contrast between MJ and JA reflects the greater penetration of cyclonic anomalies into Europe in JA. In SO, the pattern reverts to one similar to that in MJ, while in ND the extent of significant precipitation differences shrinks to a level similar to JF, with the largest precipitation differences over western Iberia.



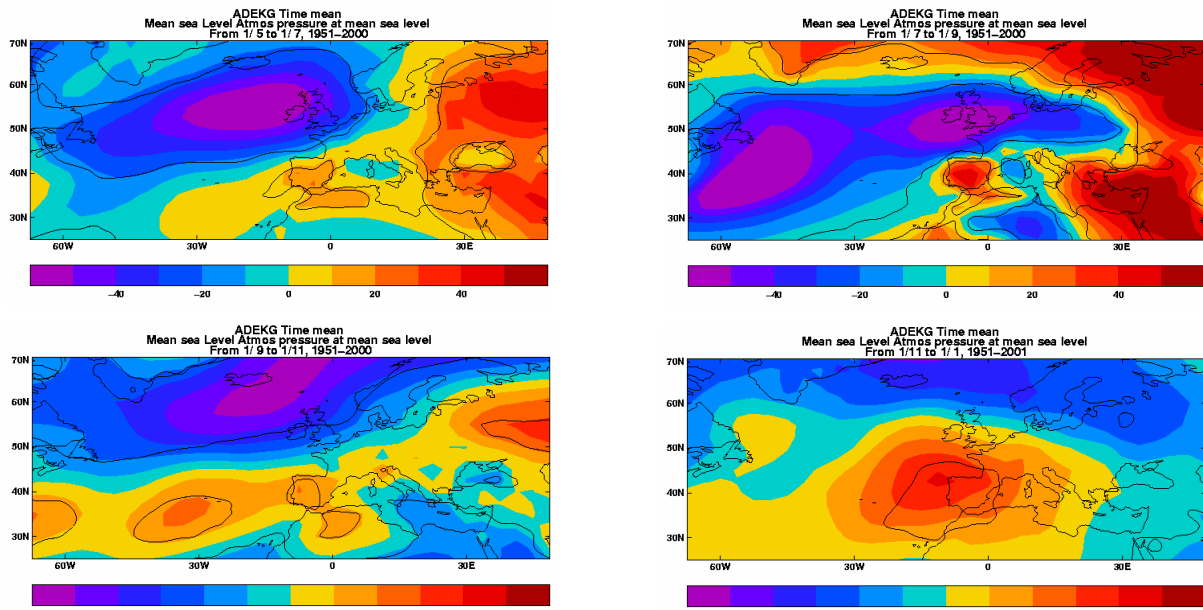


Figure 4 As figure 3 but for seasonal mslp changes. Units are Pa.

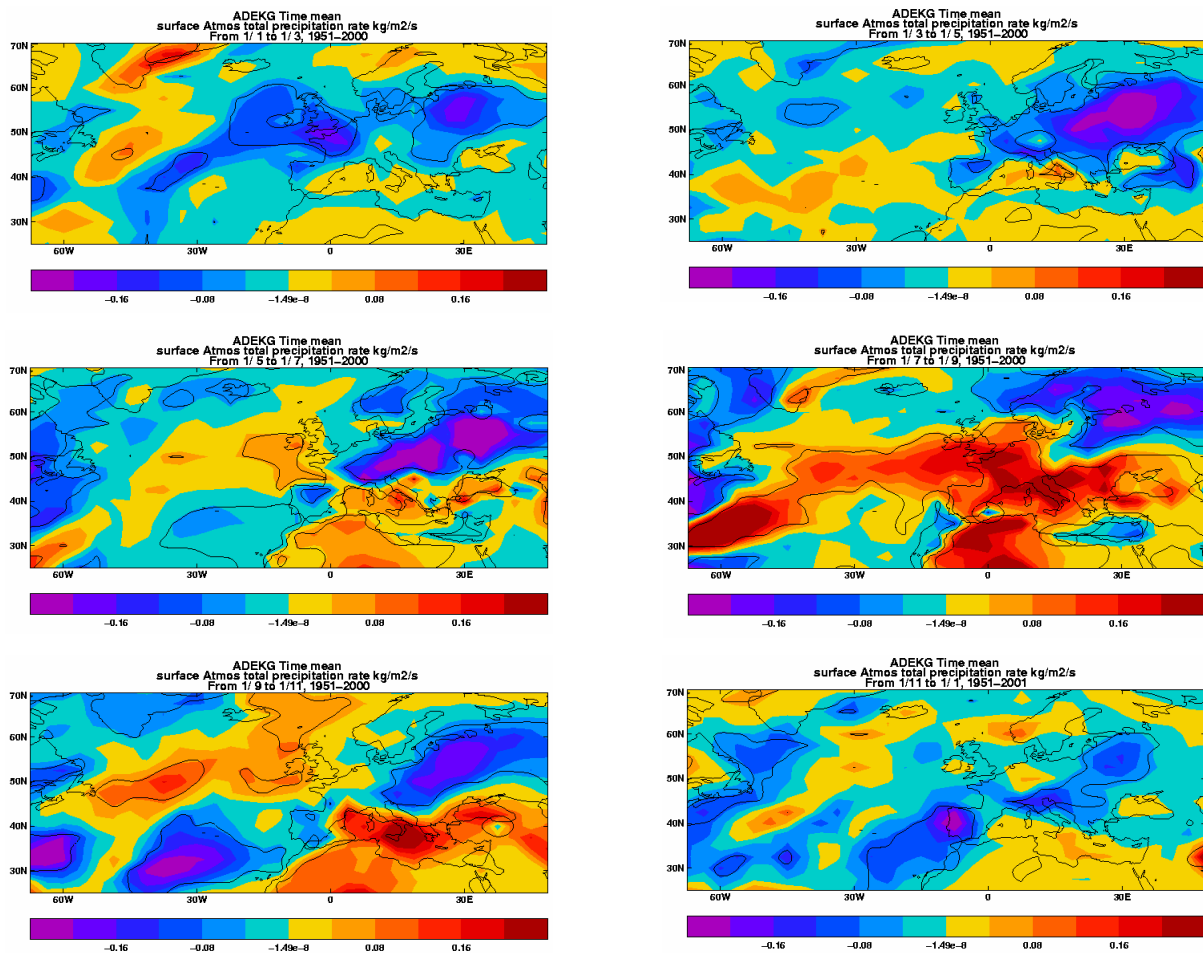


Figure 5 As figure 3 but for seasonal precipitation rate changes. Units are mm day^{-1} .

(d) *Frequencies of simulated circulation types*

We have used the model ensembles to examine the overall differences in circulation due to anthropogenic forcings by comparing mslp. Here we go further to examine the differences in the frequencies of circulation types in the simulations, ascribed by using the EMULATE classification (see D7). To apply this classification to the model results, each observed circulation type in each season is converted into an anomaly from observed climatology. Then, daily mslp anomaly patterns for each season from the simulations are classified by proximity to the observed anomalous types. Seasonal frequencies are obtained by summing the number of days of each type within the season.

To show the effect of anthropogenic forcing, we compare the distribution of mean 1950–2002 circulation types in the natural and all forcings ensembles. Those types which are significantly different are shown in figure 6. For JF, we find that type 7, showing low pressure west of Europe and high pressure over Scandinavia, occurs more frequently in the natural ensemble than in the all forcings ensemble. This is consistent with the overall bias in mslp between the ensembles, which shows a positive signal to the west of the British Isles (figure 4). No types significantly differ in MA, reflecting the relatively small mslp differences. In MJ, there is a bias towards type 8 (Scandinavian anticyclone) in the all forcings ensemble and type 2 (northeastward extension of the Azores high) in the natural ensemble. The bias in type 2 is certainly consistent with the overall mslp difference in the North Atlantic, but the origin of the positive mslp difference in Eastern Europe is less clear. The largest overall mslp effects are seen in JA, with no less than four circulation types having significant biases in this season. In particular, the prevalence of type 6 (negative summer NAO) in the all forcings ensemble is consistent with the negative overall difference in mslp between all forcings and natural ensembles. The preference of all forcings for type 1 and the preferences of natural for types 2 and 3 contribute to the positive mslp difference over Scandinavia. In SO, the biases in types 5 (towards all forcings) and 3 (towards natural) are both consistent with the negative mslp difference near Iceland. With only limited overall mslp differences, there are no significantly different circulation types in ND.

3. Simulated effect of anthropogenic forcings on European climate trends: 1951–2000

Differences in mean climate and circulation caused by anthropogenic forcings have been examined for the latter half of the 20th century using the model ensembles. We now turn our attention to differences in linear trends over this period. This period has the greatest anthropogenic influence, so is expected to produce the largest differences in trends.

(a) Surface Temperature

European mean annual temperatures in both ensembles show a downward trend before about 1985 and a subsequent increase (figure 2). Much of this is as a result of multidecadal changes in sea-surface temperatures. In terms of the difference between the ensembles, however, which corresponds to an anthropogenic influence, the overall increase between 1950 and 2002 is larger in the all forcings simulation than in the natural simulation. This largely reflects the growth in the strength of greenhouse-gas forcing and the reduction in the strength of the aerosol forcing after the 1960s.

The distribution of temperature trend differences for each two-month season is shown in figure 7. In JF, the pattern of additional warming over Europe in the all forcings ensemble mean strongly resembles the cool JF mean anthropogenic anomaly for 1951-2000 (figure 3). This indicates that the trend is towards a reduction of the aerosol-induced mean cooling over this period. On the other hand, MA, which has a similar mean climate difference to JF, shows only weak significant warming over Western Europe. MJ shows a warming signal over Eastern Europe, where the mean temperature difference is largest, but this does not spread into Western Europe where there is also a significant mean difference. A broad European warming signal is simulated in JA except for easternmost Europe and Iberia. Like MJ, SO has Eastern European warming representing a recovery of temperatures there, but little significant warming over Western Europe. Finally, in ND there is almost no significant additional anthropogenic warming.

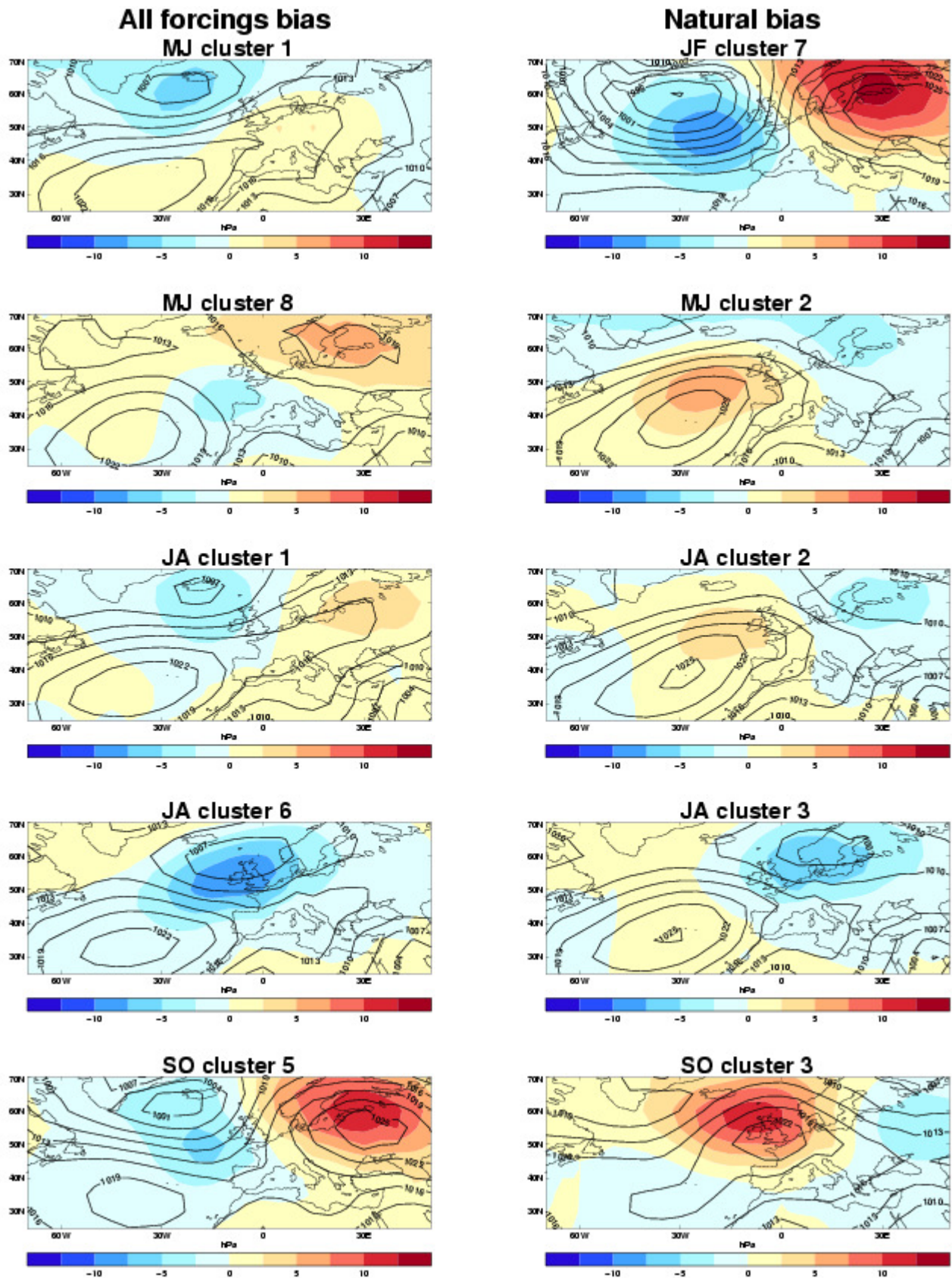


Figure 6 Circulation types showing significant (at the 90% level) differences in the 1950–2022 mean frequency of occurrence. The left-hand panels are the circulation types that are more prevalent in the all forcings ensemble. The right-hand panels are those more prevalent in the natural ensemble.

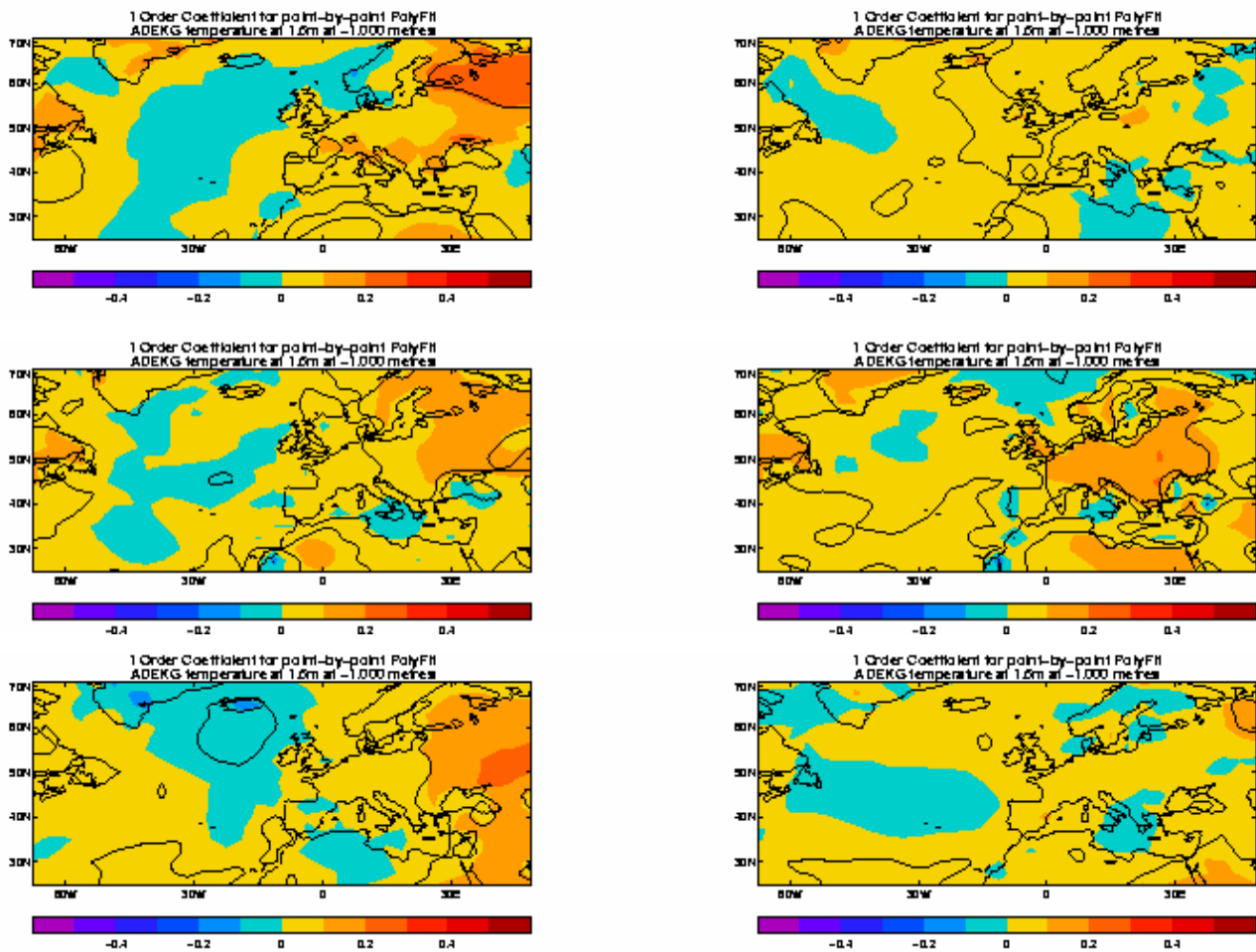


Figure 7 As figure 3, but for differences between ensemble mean 1951–2000 surface air temperature trends.

(b) Mean Sea-Level Pressure

An equivalent analysis of 1951–2002 mslp trends is shown in figure 8. The pattern of JF trends, with a centre over the UK and bands of anomalies running north-west to south-east, is approximately the opposite of the mean mslp difference for 1951–2000 (figure 4), suggesting a reduction in this bias with time. Note the observed trend of recent decades towards a more positive winter NAO is not well reproduced. The MA trends are partly similar in that the centre over Greenland and the band of opposite anomalies stretching across the Atlantic resemble a negative version of the mean mslp, but there are no trends corresponding to the anthropogenic high pressure signal over Eastern Europe. In contrast, there are almost no significant trends in MJ, except in Eastern Europe, where a trend towards lower pressure appears to be acting to reduce the positive pressure bias in the mean. There certainly does not appear to be any signal suggesting a reduction in the anomalies over the North Atlantic and North Western Europe. Further, in JA, the trend pattern (a band of mslp reductions stretching from Newfoundland across the Atlantic into Central and Southern Europe and North Africa, with mslp increases to the north) appears rather different to the pattern of mean differences, and seems to suggest increasing differences. Likewise for SO, the trends (positive over the North Atlantic and negative

over Northern Europe) seem to be somewhat aligned with the differences in mean mslp. For ND the trends are not significant, although the pattern is once more suggestively opposite to that of the mean difference. The mslp trends suggest behaviour in the cool seasons (JF, ND) rather like that which, mostly, is seen for temperature, with trends acting to diminish mean ensemble differences with time. The other seasons, however, do not show this relationship, and may even show increasing differences. Unlike surface temperature, which has something of a local radiative constraint, circulation is potentially more influenced by world-wide variations in forcing. As such, there is not the same degree of requirement for mslp trends to follow the regional forcing (figure 1); instead it could be that in some seasons the circulation is more affected by remote forcing, perhaps more akin to the greenhouse-gas dominated global forcing curve.

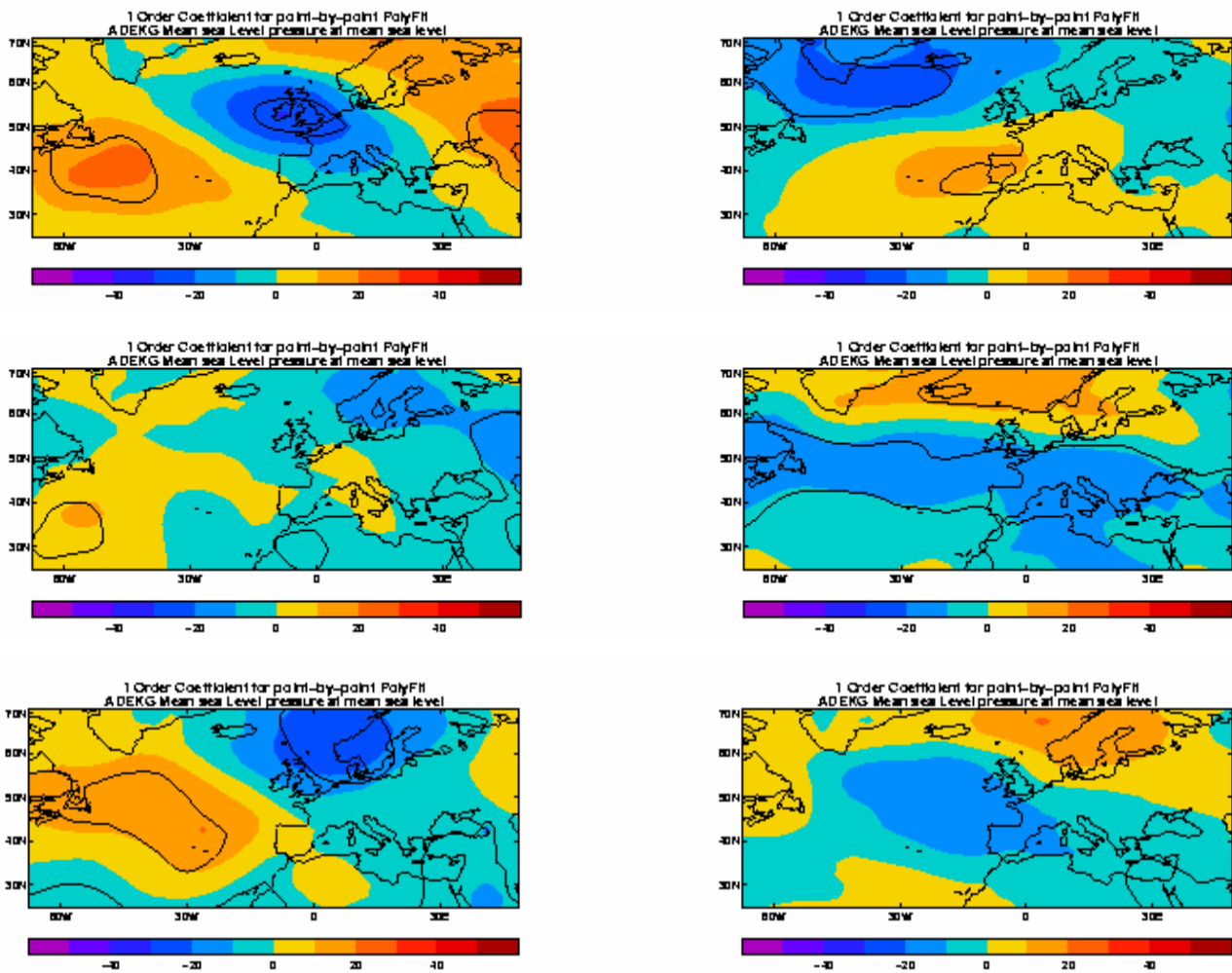


Figure 8 As figure 3, but for differences between ensemble mean 1951–2000 mslp trends.

(c) Precipitation

Just as with the 1951–2000 mean differences, the trends in precipitation follow those in mslp. As such much of the analysis

of mslp presented in the previous section applies here, except that precipitation, being inherently more 'noisy' than mslp, has less significant trends (figure 9). In fact, there are no significant large-scale precipitation anomalies across Europe, only signals that may be of regional importance, e.g. in JF over Northern France. As such, more ensemble members may help to better resolve the anthropogenic signal in precipitation trends.

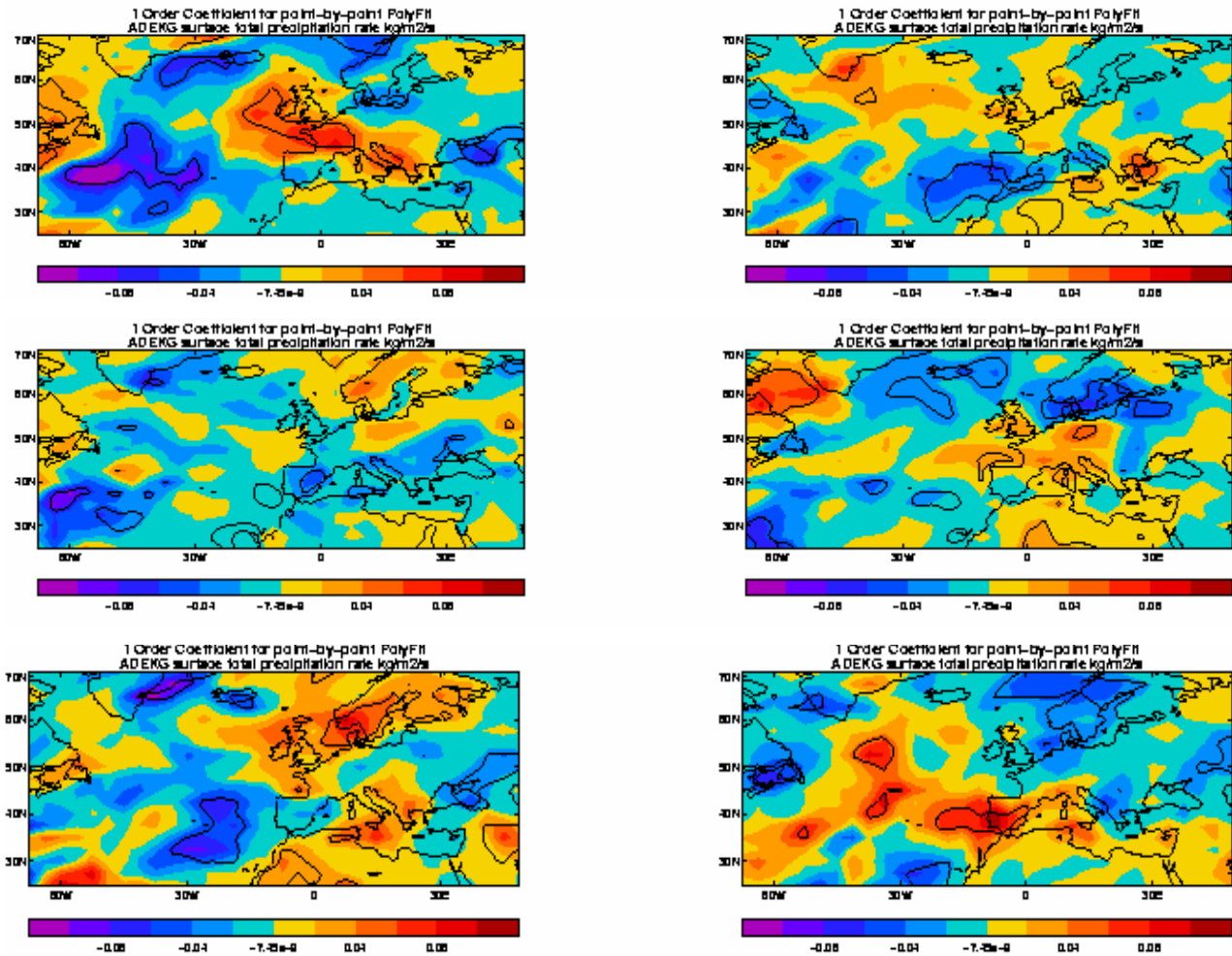


Figure 9 As figure 3, but for differences between ensemble mean 1951–2000 precipitation trends.

(d) Frequencies of simulated circulation types

Figure 10 shows the difference between the trends in circulation type frequency for each type and season (red bars). Only in two cases do the 90% limits of the estimate of this difference not include zero and so become significant (type 5 in JA and type 6 in ND). At the level of confidence used here, however, we would expect that about 5 of the 49 seasonal types would be significant just by chance. The fact that two circulation types emerge as themselves 'significant' is, therefore, not significant overall. It appears that despite the mslp trend differences seen in figure 8, there is no detectable anthropogenic signal in circulation trends in the EMULATE ensembles.

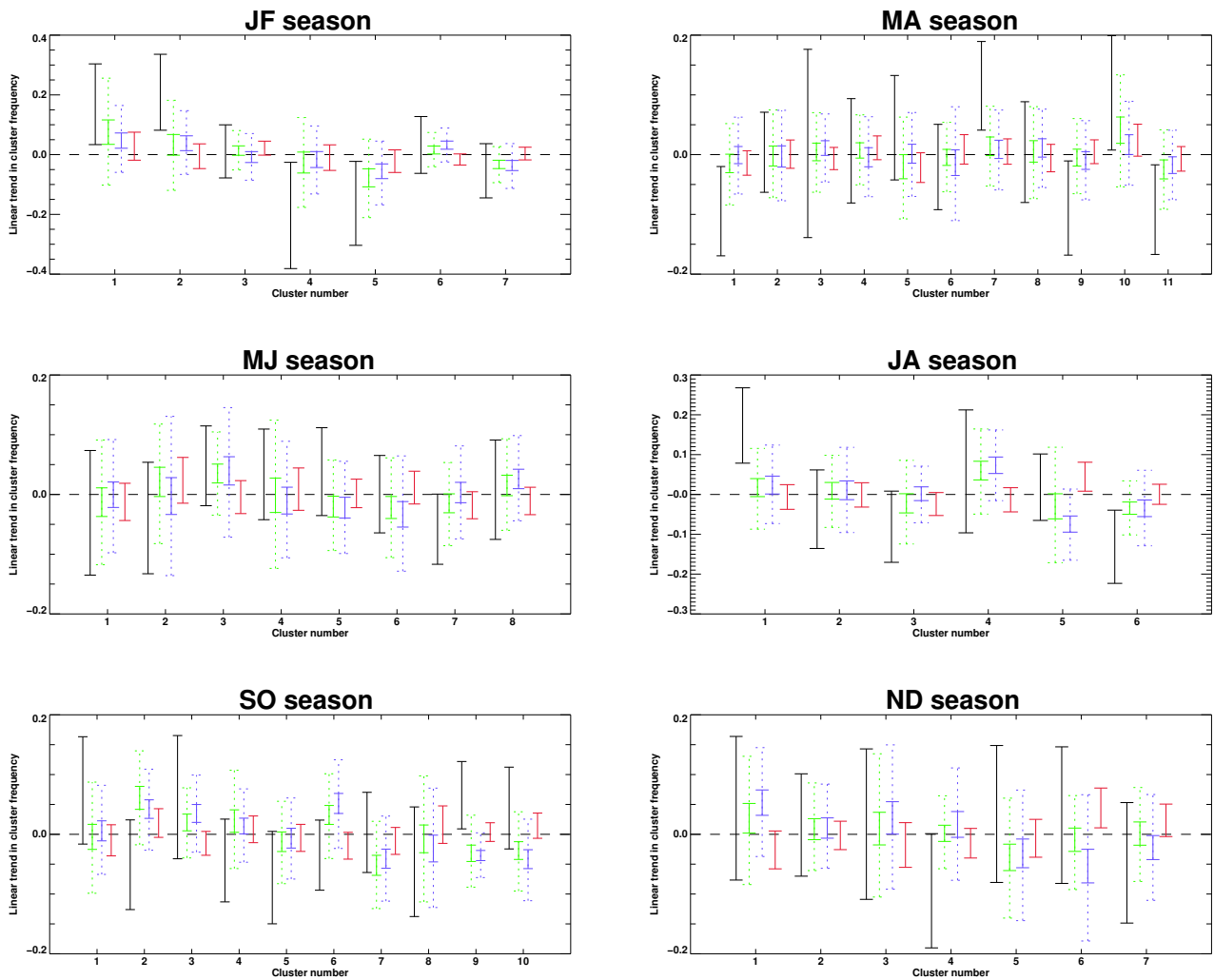


Figure 10 90% confidence intervals for linear circulation type trends for the period 1950–2002, for all two-month seasons. Trends in observed circulation type frequency (black bars), all forcings ensemble (green bars) and natural ensemble (purple bars) are shown with the 90% confidence intervals of the difference in linear trends between the ensembles (red bars). For the observed frequencies, the trend is the mean point of the bar and the 90% limits of the uncertainty in the trend are shown by the end-points of the bar. For the two ensembles, and the ensemble difference, the range of the estimated mean trend is shown by the solid bars. For the two ensembles, the 90% range of all ensemble member trends is shown by the dashed bar.

4. Attribution of circulation variability using a General Linear Model analysis

We have examined potential anthropogenic effects on circulation by looking at mean and trend differences between the all forcings and natural EMULATE ensembles. Whilst we see some mean differences, anthropogenic trends are hard to identify. It is possible to go further, however, by performing a General Linear Model analysis (Sexton *et al.*, 2003), which allows the results of the ensemble simulations to be directly related to the forcings in a statistically optimal way. This analysis also allows information about the temporal shape of the total forcing beyond a linear trend to be included.

We fitted a general linear model to the all forcing and natural ensembles of integrations for EMULATE using the method described by Sexton et al (2003). We assume a statistical model of the modelled climate variable (e.g. global mean temperature) for year y and ensemble member m ,

$$V_{y,m} = M_y + A_y + E_{y,m}, \quad (1)$$

where

M_y is the effect of mean conditions in year y (in our case this corresponds to natural forcings plus sea-surface temperature for year y),

A_y is the effect of anthropogenic radiative forcing in year y , and

$E_{y,m}$ is climate ‘noise’ with a Gaussian structure.

We first applied this general linear model (GLM) to the global mean land surface temperature in our experiments. Time series of the ensemble mean temperatures from the all forcing and natural forcing only simulations show similar values in the early part of the record but a growing difference towards the end of the 20th century (figure 11, upper left). Both ensembles increase by around 0.5 K over the last 50 years of the 20th century. Most of this overall increase in global mean land surface temperature can be explained by the mean forcings in the model that are common to both ensembles, i.e. the sea-surface temperatures and the natural forcings (figure 11, upper right). However, the GLM attributes approximately 0.1 K of the extra land surface warming in the all forcing experiments to the difference in radiative forcing; in other words, to the anthropogenic forcing (it is important to note that this is probably an underestimate of the climate sensitivity because we have used the same imposed sea-surface temperatures in both ensembles). The 0.1 K explained by total anthropogenic forcings verifies well against with the net effect of the individual forcings found in Sexton et al. (2003), where +0.42 K was attributed to greenhouse gases, -0.29 K was attributed to indirect aerosol effects, and other effects including non-linear terms were small, thereby leaving a net effect of +0.13 K. The validity of the results of the analysis depends on satisfying a null hypothesis of Gaussian residuals. Figure 12 shows the distribution of the noise values $E_{y,m}$ in this experiment plotted beside an idealised Gaussian distribution. In this case, the residuals satisfy this condition at the 99% confidence level using a Kolmogorov-Smirnov test.

We next applied the same algorithm to relate circulation type frequencies from the simulations with global mean forcing. Here it is found that the null hypothesis of Gaussian residuals could be rejected at the 99% level, implying that the analysis cannot be applied directly to circulation type frequencies. By applying a square root transformation to the circulation type frequencies, however, the data becomes sufficiently Gaussian that we can no longer reject the null hypothesis. Hence GLM analysis was

performed on this transformed data. We calculated the contribution of anthropogenic forcing to the changes for all circulation types which showed a strong trend or systematic difference between the all forcing and natural forcing ensembles (see above). The circulation types are as follows - JF: 7; MJ: 1, 2, 8; JA: 1, 2, 3, 5, 6; SO: 3, 5; ND: 6. An example is shown in figure 13 where again, the majority of the variability can be explained by the mean forcing effect from sea-surface temperatures and natural forcings.

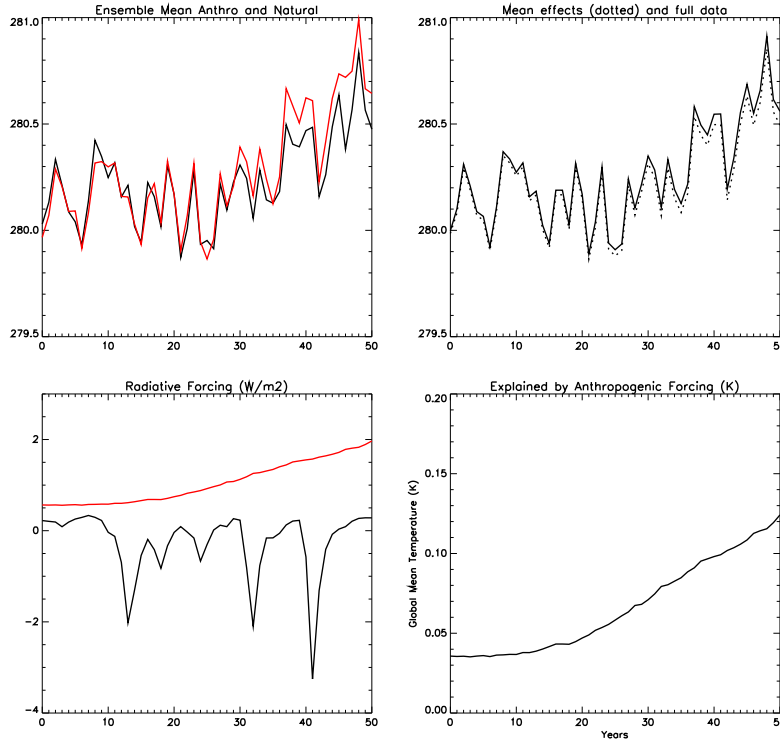


Figure 11 GLM analysis of global mean land surface temperature for 1950-2000. Upper left, Ensemble mean temperatures for all forcing (red) and natural forcing only (black) ensembles. Upper right: Mean GLM effects (M_y , dotted) and full ensemble mean data (solid). Lower left: Anthropogenic forcing (red) and natural forcing (black). Lower right: changes in surface temperature statistically attributed to anthropogenic forcing.

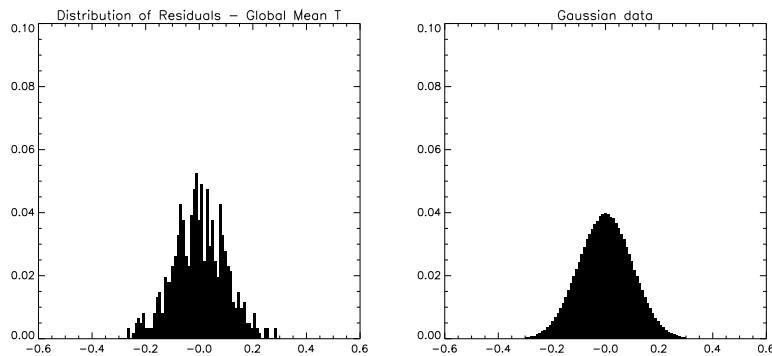


Figure 12 Distribution of temperature residuals from equation 1 (left panel) and idealised Gaussian test data with same mean and standard deviation for comparison using the Kolmogorov-Smirnov test (right).

Only a very small residual is explained by the anthropogenic forcing and this is much less than the interannual variability in circulation type frequency. This is perhaps not surprising given the large amount of climate noise in circulation type frequencies (figure 14). A qualitatively similar picture emerges for all the circulation types we tested and it is difficult to pick out clear, large anthropogenic effects on any of the circulation type frequencies, at least from global mean forcing.

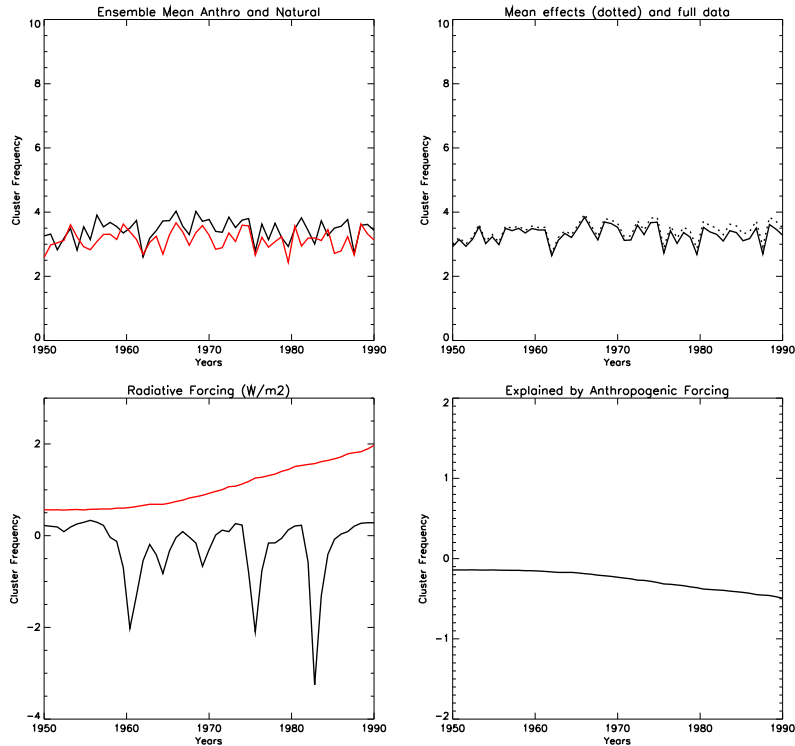


Figure 13 GLM analysis of square root circulation type frequencies for July-August circulation type 2. Upper left, Ensemble mean square root frequencies for all forcing (red) and natural forcing only (black) ensembles. Upper right: Mean GLM effects (M_y , dotted) and full ensemble mean data (solid). Lower left: Anthropogenic forcing (red) and natural forcing (black). Lower right: changes in square root circulation type frequency statistically attributed to anthropogenic forcing.

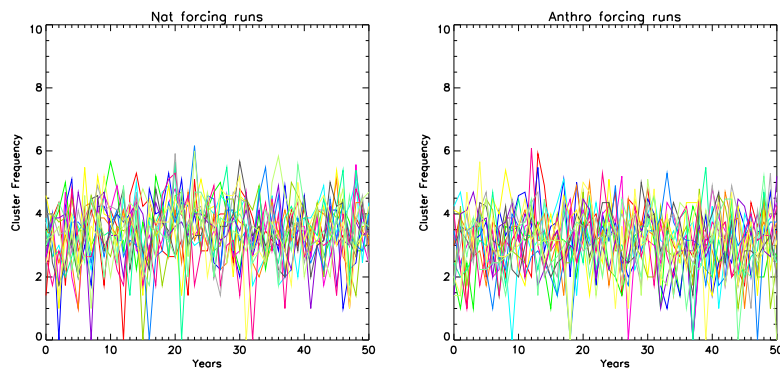


Figure 14 Circulation type frequencies in individual simulations for July-August circulation type 2.

5. Effects of volcanic and solar variability on simulated European climate

Until now we have focussed on the differences between the all forcings and the natural ensembles to infer the effects of forcings on European climate, especially circulation. This gives an assessment of the integrated effects of all the anthropogenic forcings. It would also be useful to quantify, however, the effects of solar and volcanic forcings, which are the principal natural forcings.

(a) Volcanic forcing

For volcanic forcings, we follow Jones *et al.* (2003), who used superposed epoch analysis on observed surface temperature data to infer the influence of volcanic eruptions on regional and mean Northern Hemisphere temperature. Their results indicate a significant reduction in mean Northern Hemisphere temperature in the warm seasons of the two years following an explosive tropical eruption. An effect is also seen in the late summer of the eruption year for extratropical eruptions. There are less clear responses, however, in more regional temperatures.

The superposed epoch analysis works by simply averaging 10-year sections of data centred on each of the known volcanic years lying within the period for which we have data. In our ensembles, volcanic signals can be transmitted through direct radiative forcing or through the effect of eruptions on historical sea-surface temperatures used to force the model. Using the natural ensemble, we compute ensemble mean temperatures for 1870–2002 and then remove low-frequency components with time scales longer than 30 years. We then superpose the data centred the volcanic years, having subtracted the mean of the 5 pre-volcanic years in the case of each eruption. For tropical eruptions, the eruption years are 1883, 1902, 1963, 1982, and 1991, and for the extratropical eruptions, the years are 1907, 1912, and 1956. To perform significance testing, a large number of superposed epochs, each based on a number of random years equal to the number of eruptions, are computed.

The results of the analysis of the effect of tropical volcanic eruptions on simulated Northern Hemisphere mean temperature (not shown) essentially confirm the results of Jones *et al.* (2003). Using a model ensemble in place of observations, which correspond to a single realisation of the variable climate, improves the significance of the signals. We see cooling in the two years following the eruption year almost year-round, but with its largest effects in summer. The results for the extratropical eruptions, however, do not show cooling in any year. In fact, none of the analyses performed show any response to the extratropical eruptions, so will not be mentioned further.

For European regions such as Central England and Central Europe, Jones *et al.* (2003) failed to find a volcanic signal, although for Fennoscandia they showed a marginally significant tendency for winter warming and summer cooling. Similarly, we are unable to detect any significant effect in European mean temperatures in a single ensemble member. Using the ensemble mean European temperature, however, allows the forced signal to be identified (figure 15), implying there is too much noise in a single

realisation of climate to detect any significant effect in European mean temperatures. The results confirm a cooling effect in the warm seasons. For MJ the year after the eruption is significantly cooler than average, while for JA this is also true for the second year after the eruption. SO shows a post-volcanic cooling that is marginal in significance in the first and second years after the eruption. No significant effects are seen in JF, MA and ND, and in particular there is no winter warming signal. If this warming is dynamically induced, however, this result may be sensitive to the domain of the region over which temperatures are averaged. Nevertheless, these results confirm that on average explosive tropical volcanic eruptions are expected to cool Europe in the summer, even though interannual variability can mask the effect of an individual eruption.

The superposed epoch methodology can be used to examine possible volcanic effects on European circulation by superposing data for seasonal circulation type frequency for observations (see D7), and for the 1870–2002 ensemble mean from the simulations (derived as described above). For the analysis of the effect of tropical eruptions on observed frequencies, no systematic effects were seen (not shown). Occasionally, frequencies for some years in some months just reach the 95% significance level, but this would be expected by chance given the large number of seasons, circulation types and post-volcanic years examined. Our inability to detect a signal in observed circulation mirrors the results for observed European mean temperature.

We might hope that the use of the model ensemble would allow a clearer detection of circulation signals. Unfortunately, the results show almost no significant effects in any season. An example for the JA season, which shows the largest temperature effects, is shown in figure 16. Perhaps the most suggestive circulation frequency change is for type 3 (low pressure anomalies over Northern Europe), which appears to decline after tropical eruptions, just reaching the significance level in the second year after the eruption. This significance is marginal, however, and overall the effect is not entirely convincing. The frequencies of types 2 and 5 similarly seem to show changes without being clear signals. These results show that for the model, at least, the circulation effects of tropical volcanic eruptions are small compared to the considerable interannual variability in European circulation.

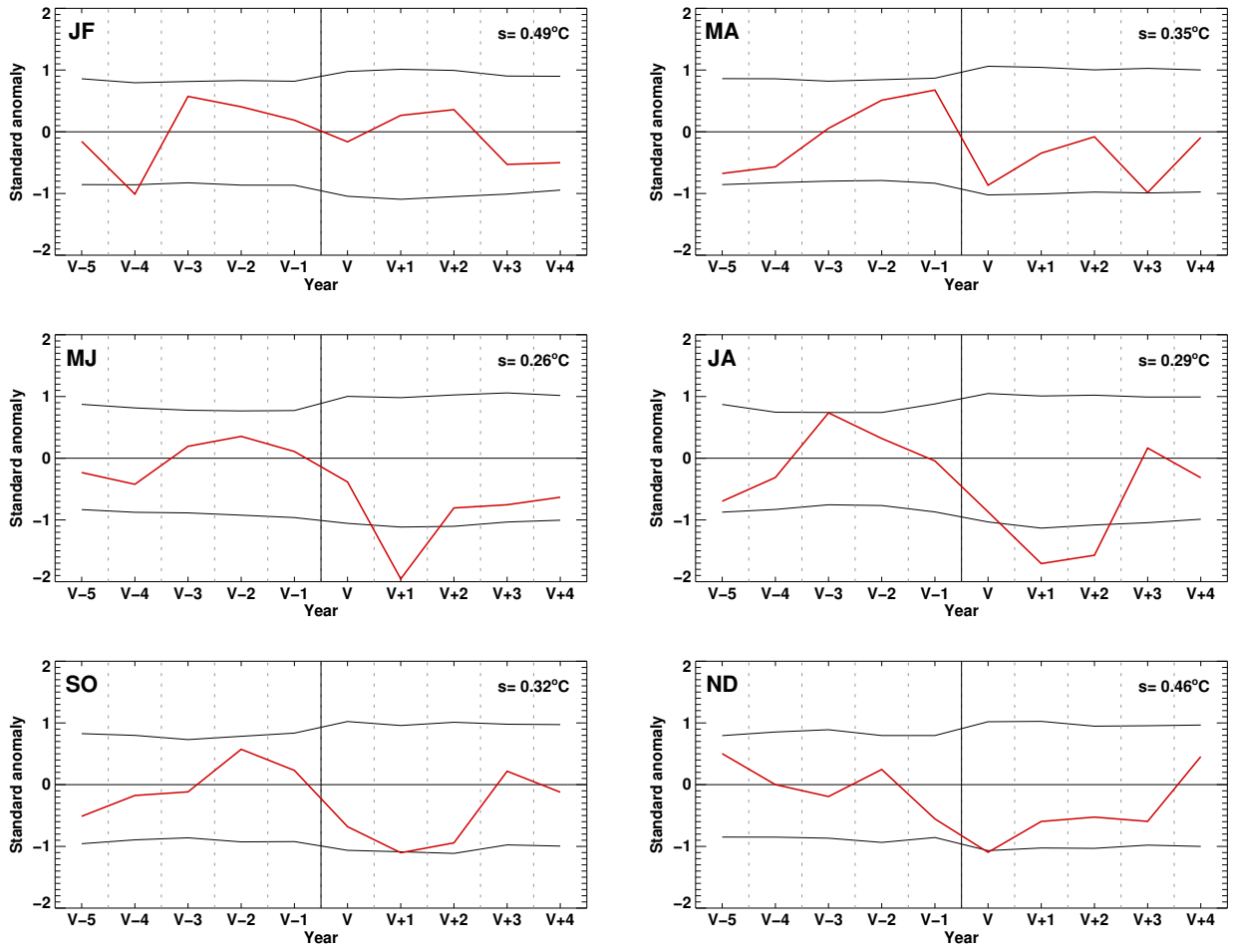


Figure 15 Superposed epoch analysis of European mean (30°W - 60°E , 35° - 70°N) land air temperatures for tropical volcanic eruptions (red). 5% significance limits are shown as black curves. Years are referred to relative to the eruption year (V). Units are standard anomalies of 30-year low-pass filtered ensemble mean temperature. The value of the standard deviation in each season is printed at the top right of the panel.

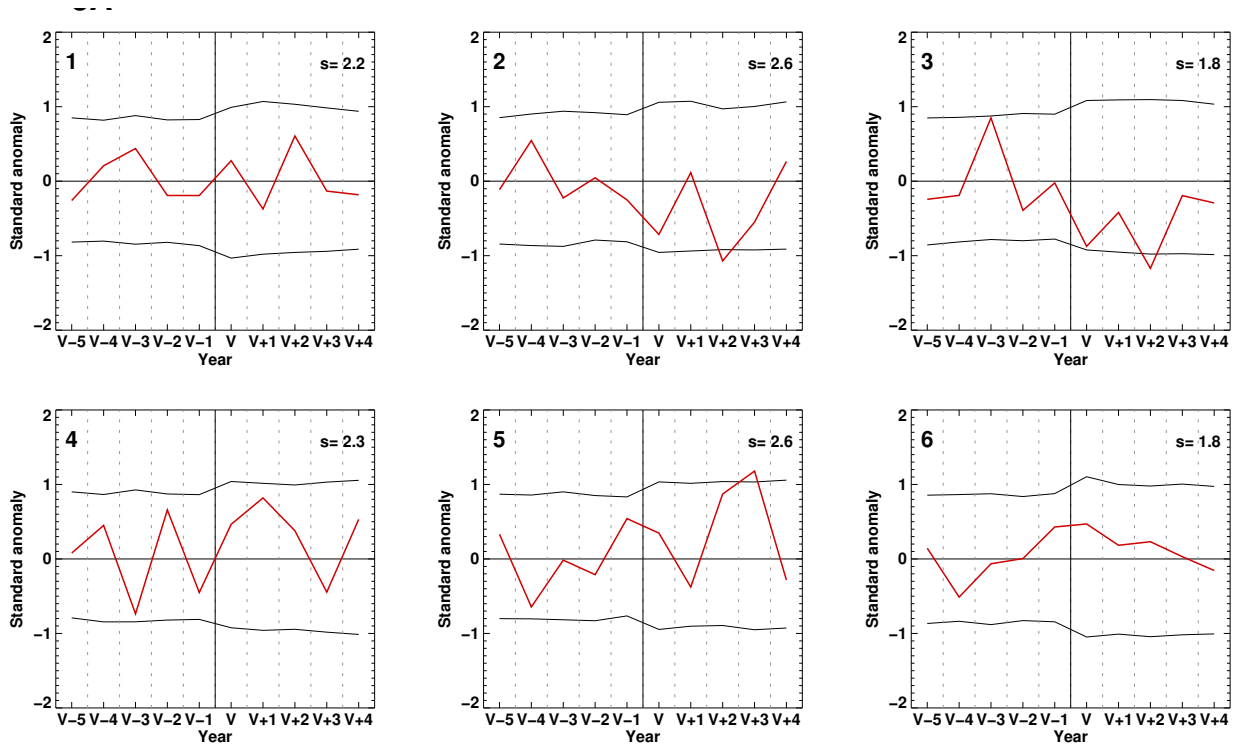


Figure 16 As figure 15, but for frequencies of the six simulated circulation types for the JA season. The circulation type number (see D7) is shown in the top left of each panel.

(b) Solar forcing

The solar forcing in the model is described in Stott *et al.* (2000). Briefly, it comprises two parts - an 11-year solar cycle and longer term variations. As well as total solar irradiance changes, larger changes in the shorter wavelength solar radiation are included. The longer time scale variations happen to be correlated with the global mean of the sea-surface temperature changes applied in the simulations, making it impossible to separate the solar and sea-surface temperature effects on climate. Other results, such as the Stott *et al.* (2000) work, show that possible long term increases in solar irradiance may have had a warming effect globally in the early part of the 20th century. The 11-year solar cycle component is more amenable to study with the EMULATE simulations. We have correlated the total solar irradiance time series, filtered to remove variations on time scales longer than 30 years, with observed European mean temperature. No significant relationships are found. For the ensemble mean of the natural ensemble, however, there is the suggestion of relationship in summer (MJ and JA). For example, filtered JA mean European temperature is compared to the solar cycle irradiances in figure 17. Clear periods can be seen where the temperature on roughly decadal time scales is strongly correlated with solar irradiance, although at other times the link is less clear. Overall, taking account of autocorrelation, the irradiance-temperature correlation is +0.32, significant at the 95% level. Some care must be taken in the interpretation of these results as the solar forcing may be aliased onto the volcanic forcing or sea-surface temperature signals, reducing our ability to attribute changes to a single cause.

Simulated frequencies of occurrence of circulation types were also tested for a solar influence. Two types produced apparently significant changes at the 90% level - type 4 of MJ and type 5 of SO. The overall number of circulation types through the year is sufficiently high (49), however, that we would expect to find about 5 correlations that appear significant at the 90% level just by chance. As such, factors producing about this or fewer 'significant' links with circulations types are not considered significant overall. Thus we conclude that there is no significant effect of solar cycle irradiance changes on European circulation.

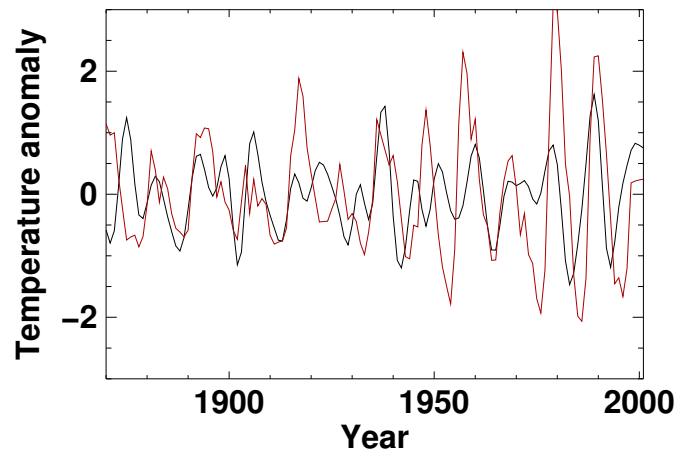


Figure 17 Comparison of simulated JA mean European temperature (black) with solar irradiance (red). Both series have been filtered to remove low-frequency variations with time scales greater than 30 years. Additionally, the temperature series is filtered to remove sub-decadal variations. Units for temperature anomalies are in $^{\circ}\text{C}$, while units for solar irradiance are in W m^{-2} .

6. Future trends in the summer NAO.

The summer NAO is the principal mode of observed climate variability over North West Europe in high summer (JA). The D7 and D11 reports document its manifestation in the circulation type classification and its links with climate and sea-surface temperature. In this report we have shown that the ensembles imply an effect of anthropogenic forcing on the summer NAO. Here, we extend our modelling studies using analyses performed jointly with the FP6 project DYNAMITE (contract 003903-GOCE), examining the summer NAO in simulations of future climate. The simulations were performed with the first version of the Hadley Centre Global Environmental Model (HadGEM1), which couples ocean and ecosystem models with an atmosphere model. Simulations used are a control, with no changes in external climate forcing, a $2\times$ CO_2 simulation and a $4\times$ CO_2 simulation. For the transient CO_2 simulations, CO_2 increases from its pre-industrial concentration (~ 280 ppmv) by 1% per year for 70 and 140 years respectively, reaching double and quadruple levels of CO_2 , and then remains constant. These levels were chosen as they roughly span the range of concentrations

expected by the year 2100. All other forcings other than CO₂ remain constant.

We examined the interannual variability of the summer NAO by performing a Principal Component Analysis of JA mslp from the control integration (not shown). This shows that the HadGEM1 model possesses a realistic summer NAO, with out-of-phase variations in pressure with centres near North West Europe and Greenland. Using the control simulation as a guide, we defined an index of the summer NAO as the difference in mslp between the points (5°E, 60°N, [North West Europe]) and (35°W, 70°N, [Greenland]). This index was computed for the control, 2× and 4× CO₂ simulations. The difference between the summer NAO index in the transient simulations relative to its mean value in the control is shown in figure 18, alongside the CO₂ concentration in each simulation. Despite multidecadal variability, this shows that for a doubling of CO₂ the mean summer NAO is indeed higher (by about 2 hPa) than the mean in the control simulation. This change is roughly similar to the entire observed change in the summer NAO since 1850. The summer NAO in the quadruple CO₂ simulation is about a further 2 hPa higher. The shape of the change largely mirrors that in the CO₂ concentration, increasing rapidly in the years when CO₂ is increasing and then more gradually. These results imply an increasingly positive summer NAO driven by increasing CO₂. Further, there is a steady progression towards a more positive summer NAO as with increasing CO₂, suggesting increased anticyclonic circulation over North West Europe in the future as CO₂ levels rise. This could lead to more frequent occurrence of summer drought conditions in this region.

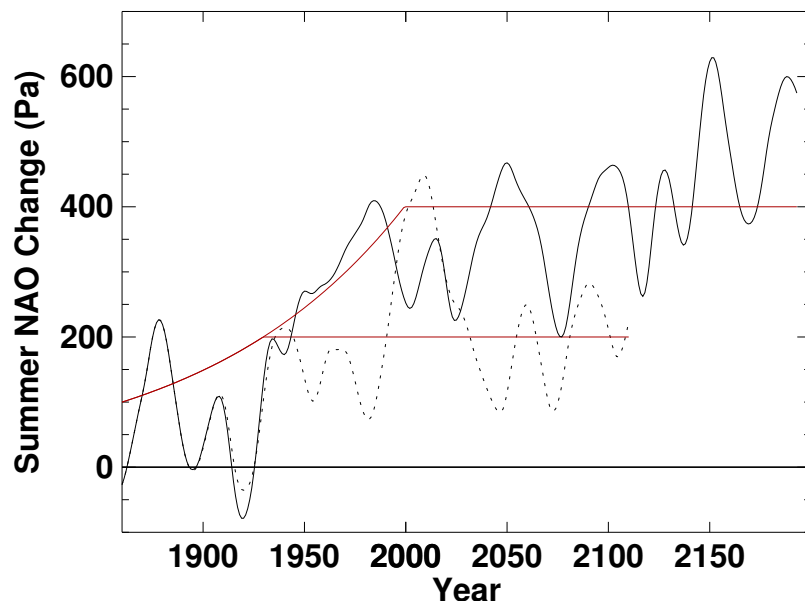


Figure 18 Variations in the summer NAO index for 2× (dashed) and 4× (solid) CO₂ simulations. In each case the index has been filtered to retain variability with periods longer than 30 years. Values shown are relative to the mean value in the control simulation. CO₂ concentrations (ppmv) for the two simulations are shown in red, with a scaling of 1/2.8.

7. Conclusions

This report has focussed on work within workpackage 3 of EMULATE to identify responses to climate forcings and the role of internal variability in European climate. To do this, we have first examined two ensembles of climate model simulations with different sets of forcing factors - one with the major natural forcings and one with both natural and anthropogenic forcing factors. Comparison of these two ensembles of simulations has allowed, within the limits of statistical uncertainty, some of the effects of anthropogenic forcings on European climate, including circulation, to be evaluated.

We find that the mean 1951-2000 simulated temperature over Europe is reduced by, on average, about 0.5 °C, due to the cooling effect of anthropogenic aerosols. As such, Europe responds differently to much of the rest of the globe, which shows a mean anthropogenic warming over this period. The effect appears to be strongest in Eastern Europe in the cold half of the year, but strongest in Western and Southern Europe in the warm half of the year. The only exception to this is for Northern Scandinavia, which is warmed in winter by anthropogenic forcing. These patterns can be understood by the action of anthropogenic aerosols in reflecting solar radiation; for most of Europe, the largest cooling occurs in summer, when the solar radiation peaks. In Eastern Europe there is a snow cover feedback on temperature, causing the most cooling to occur there in winter.

Linear trends in temperature tend to show the simulated mean 1951-2000 anthropogenic cooling diminish over time. For the European mean temperature, this reflects initial relative cooling, and subsequent relative warming, resulting in similar temperatures in both ensembles by 2000. This pattern is consistent with that in the mean European climate forcing, which shows a minimum in the 1960s. In identifying an anthropogenic cooling effect, we recognise that by using simulations with sea-surface temperatures specified from observations it is only possible to detect the part of the anthropogenic effect that does not come from sea-surface temperature. Any anthropogenic warming arising from sea-surface temperatures will, therefore, diminish the overall anthropogenic European cooling. Nevertheless, the greater size of the negative forcing signal over Europe compared to the positive signal globally suggests that sea-surface temperature effects will be secondary. Further tests to quantify this fully could be done with coupled models, although because Atlantic Ocean internal variability is large, this would imply large ensemble sizes. Hybrid simulations, which couple the atmosphere model to the full dynamical ocean model except in chosen regions (where a near-surface model is used), may help to overcome this problem (Kinter *et al.*, 2006).

Although the role of aerosols has diminished, such that future forcing trends are expected to be dominated by greenhouse-gas emissions, these results show that it is important to take into account aerosol cooling when attributing past European climate variability, e.g. the cold winters of the 1960s. Uncertainty in the amount of cooling might arise from sea-surface temperatures, as stated above, and from the representation of aerosol in the model. Further, the contribution of natural aerosols is uncertain, making attribution of anthropogenic forcing less clear. Estimates of man-made aerosol radiative forcing are also uncertain

(Ramaswamy *et al.*, 2001). Although these uncertainties are considerable, the magnitude of the effect is large enough to make some degree of anthropogenic cooling in European climate in the latter half of the 20th century likely.

Overall circulation responses, as measured by ensemble differences in mslp, show a seasonal response, with the largest changes in summer and smallest changes in winter. In summer the anthropogenic effect appears to be a pattern over North West Europe similar to that associated with the negative phase of the observed summer NAO. Additionally, there are increases in mslp over Eastern Europe. Impacts in winter are not as generally significant as in summer, although there does appear to be significant increases in mslp over Western Europe. The lack of strong forced signals in winter, which has large total variability, shows the importance of internal variability. In terms of trends, winter mslp changes are reminiscent of temperature, in that they act to reduce the time mean differences, whereas summer trends have quite different patterns to the 50-year means, and in some places suggest a growth in mean differences. This arises because European circulation can respond to remote forcings, whereas surface temperature is more constrained by the regional radiation balance. The anthropogenic effects on precipitation largely mirror those in mslp, with elevated precipitation associated with reduced mslp. Signals vary through the year, but perhaps the largest effect is in high summer (JA), which shows higher precipitation throughout Western and Southern Europe.

Anthropogenic impacts on circulation have also been examined using the EMULATE circulation type classification, developed in workpackage 2, and applied to the mslp results from the simulations. Mean 1951-2000 circulation type frequencies confirm the view that the largest circulation effects are seen in the warmer seasons. Of particular note are the shifts in 4 of the 6 types for high-summer (JA), including the type corresponding to the negative summer NAO. Differences in trends in circulation type frequency, however, appear not to be significant overall, with only 2 significant types amongst the 49 annual types - less than would be expected by chance. This suggests that there is considerable internal variability in circulation type frequency. This view is confirmed by a General Linear Model analysis, which fails to relate apparent circulation frequency changes to global mean anthropogenic forcing, despite showing a clear link between global mean temperature and forcing. It remains possible, however, that this test may reveal more information when applied using European regional forcing.

In addition to anthropogenic forcing, we have attempted to diagnose the effects of natural forcings in our simulations. Using a superposed epoch analysis we show that there is summer cooling typically of order 0.4 °C over Europe in the first and second years after the year of a major tropical explosive eruption. We do not find the suggested winter warming signal in our simulations, or any effects of extratropical eruptions. For circulation, there is little suggestion of a change in the simulated frequencies of circulation types after either kind of eruption. The most marginal case is again for summer, which perhaps shows a prevalence of types with low pressure over Northern Europe after tropical eruptions. Correlations of European ensemble mean temperature with the 11-year solar cycle also show an effect in summer of a few

tenths of a °C. We find no significant solar cycle effect, however, on circulation.

Overall, the most significant forced signals found in this study are in the warm seasons, particularly in JA. The responses partly appear to be manifest as changes in the summer NAO, the leading mode of observed JA summer variability. We examined possible future changes in the summer NAO by extending our use of modelling simulations to include double and quadruple CO₂ experiments using a coupled model. These levels of forcing are expected to be realistic for perhaps the mid- to late-21st century. Progressive changes in the summer NAO were found with increasing CO₂ that would increase summer mslp over North West Europe. This suggests a heightened risk of summer droughts in this region in the future, additional to that from increased evaporation associated with projected warming.

Further work to better characterise the role of forcings on circulation might involve looking at responses in other models. The results here are only from a single model and may, to some extent, be model-dependent. In addition, it would be useful to quantify any component of the anthropogenic effect on European climate that arises from anthropogenic sea-surface temperature changes. One approach would be to use coupled model simulations, or hybrid simulations in which internal ocean variability could be partially excluded. These were not the priority in EMULATE because we also aimed to study the effect of realistic sea-surface temperature variations on European climate. Another approach would be to attempt to remove anthropogenic sea-surface temperature signals from the imposed sea-surface temperatures, perhaps by using off-line coupled simulations. For some of the forcings, such as solar cycle variability, there is some uncertainty over the direct attribution of apparently correlated climate signals because multiple forcings may be aliased together. Single-forcing simulations may resolve this problem. Furthermore, in EMULATE we have taken the approach of seeking the variability and change in European circulation and then relating it to the major outside influences in the climate system, such as climate forcings, North Atlantic sea-surface temperatures, El Nino-Southern Oscillation variability etc. Another approach, as used in the FP6 DYNAMITE project, is to study variability and change in these principal global phenomena and then ask how this relates to European climate.

References

Folland, C. K., et al. (2002), Observed climate variability and change, in *Climate Change 2001: The Scientific Basis - Contribution of Working Group I to the Third Assessment Report of the Intergovernmental Panel on Climate Change*, edited by J. T. Houghton et al., pp. 99-181, Cambridge Univ. Press, New York.

Johns, T. C., J. M. Gregory, W. J. Ingram, C. E. Johnson, A. Jones, J. A. Lowe, J. F. B. Mitchell, D. L. Roberts, D. M. H. Sexton, D. S. Stevenson, S. F. B. Tett, and M. J. Woodage (2003), Anthropogenic climate change for 1860 to 2100 simulated with the HadCM3 model under updated emissions scenarios, *Clim. Dyn.*, 20, 583 - 612.

- Jones, P. D., A. Moberg, T. J. Osborn, and K. R. Briffa (2003), Surface climate responses to explosive volcanic eruptions seen in long European temperature records and mid-to-high latitude tree-ring density around the northern hemisphere, in *Volcanism and the Earth's Atmosphere*, edited by A. Robock, pp. 239-254, American Geophysical Union, Washington.
- Kinter, J., C. K. Folland, and B. Kirtman (2006), Pacemaker experiments and the Climate of the Twentieth Century Project. Submitted to *CLIVAR EXCHANGES*.
- Pope, V. D., M. L. Gallani, P. R. Rowntree, and R. A. Stratton (2000), The impact of new physical parametrizations in the Hadley Centre climate model: HadAM3, *Clim. Dyn.*, **16**, 123-146.
- Ramawsamy, V., et al. (2002), Radiative Forcing of Climate Change, in *Climate Change 2001: The Scientific Basis - Contribution of Working Group I to the Third Assessment Report of the Intergovernmental Panel on Climate Change*, edited by J. T. Houghton et al., pp. 99-181, Cambridge Univ. Press, New York.
- Rayner, N. A., D. E. Parker, E. B. Horton, C. K. Folland, L. V. Alexander, D. P. Rowell, E. C. Kent, and A. Kaplan (2003), Global analyses of sea surface temperature, sea ice, and night marine air temperature since the late nineteenth century. *J. Geophys. Res.*, **108**, 4407, doi: 10.1209/2002JD002670.
- Scaife, A. A., J. R. Knight, G. K. Vallis, and C. K. Folland (2005), A stratospheric influence on the winter NAO and North Atlantic surface climate, *Geophys. Res. Lett.*, **32**, L18715, doi:10.1029/2005GL023226.
- Sexton D. M. H., H. Grubb, K. P. Shine, and C. K. Folland (2003), Design and analysis of climate model experiments for the efficient estimation of anthropogenic signals, *J. Climate*, **16**, 1320-1336.
- Stott, P. A., S. F. B. Tett, G. S. Jones, M. R. Allen, J. F. B. Mitchell, and G. J. Jenkins (2000), External Control of 20th Century Temperature by Natural and Anthropogenic Forcings, *Science* **290**, 2133-2137.